Frequency Scanning Leaky-wave Slot Antenna Array Based on Serpentine Waveguide with Open Stopband Suppression

Álvaro Jaque, Gerard Zamora, *Member, IEEE*, and Jordi Bonache, *Member, IEEE*

***Abstract*— A periodic leaky-wave antenna with backward to forward scanning capability is presented. Two versions of the antenna, one with bi-directional radiation and the other with unidirectional radiation are introduced. The proposed structure, composed of 30 unit-cells (UC), is based on a meandered rectangular waveguide loaded with transverse radiating slots. Effective suppression of the open stopband is achieved allowing for efficient broadside radiation at 5 GHz. Measured and simulated S-parameters, radiation pattern, and gain are reported. The experimental results demonstrate a backward to forward scanning capability from −35° to 42° for both the unidirectional and bidirectional versions, with a maximum measured gain of 15.5 dB and 16.5 dB, respectively.**

***Index Terms*—Leaky-wave antenna (LWA), waveguide, bi-directional radiation pattern, frequency scan antenna (FSA).**

I. Introduction

LEAKY-WAVE ANTENNAS (LWAs) have been one of the most active areas of research in microwave engineering since the 40's due to their ability to achieve high directivity, narrow beamwidth over a wide frequency band and beam scanning capability [1]. These devices are based on a wave propagating along a guiding structure and gradually leaking its energy out to free space. Leaky-wave antennas are generally divided into two categories depending on the geometry: uniform (or quasi-uniform) and periodic. In uniform LWAs the guiding structure is homogeneous along its length and supports a fast wave with respect to free space. Quasi-uniform LWAs operate in a similar way as uniform LWAs, except that a periodic guiding structure is used. In periodic LWAs the guiding structure exhibits a periodic perturbation and supports a slow wave. In this case, the periodic perturbation generates infinite space harmonics, some of which are fast and can radiate. Periodic LWAs are normally designed to radiate with the $n = -1$ space harmonic. Whereas uniform LWAs can only radiate in the forward quadrant, quasi-uniform (based on composite right/left-handed transmission lines) and periodic LWAs have beam-scanning capability from the backward to the forward quadrant, effectively radiating through broadside [2].

The main common problems to deal with in the design of periodic LWAs are the appearance of the open stopband (OSB), that degrades the radiated beam around broadside, and the emergence of grating lobes in the radiation pattern. Commonly used techniques to eliminate the grating lobes are reducing the interelement spacing [2] or using spatial filters [3]-[4]. Regarding the open stopband phenomenon, different approaches have been proposed to mitigate or eliminate its presence. One of the common techniques is to load the unit cell with an extra radiating element per unit cell distanced $\lambda_g/4$ (λ_g being the guided wavelength at the broadside frequency) from the original radiation element [1], however this technique usually tends to mitigate its effects, but not eliminate them completely. Recently, more innovative methods have been proposed to deal with OSB phenomenon [5]-[11]. In [5], two non-identical slots are used in each unit cell, achieving OSB mitigation. In [6] a combination of dispersion enhancement and meandered unit cells is proposed to realize leaky-wave antennas with very high scan rates, yielding good results in OSB mitigation. However, these works focus on traveling-wave frequency scanning antenna arrays based on dielectric-filled structures.

In a traveling-wave frequency scanning antenna array, generally there are two basic approaches [3],[12]: designs loaded with dielectric materials, resulting in slow wave radiation, and designs based on hollow or air-filled structures, which result in fast wave radiation. Dielectric structures allow for compact designs, and easy integration into PCB when they are based on planar technologies. However, dielectric-filled structures are limited in the amount of power they can handle and are highly sensitive to environmental conditions such as temperature or humidity [2], [13], [14]. Air-filled waveguide based periodic LWAs are a good option for scanning applications where high-power handling capability, low loss, good stability, and reliability is required [13]-[15]. The serpentine arrangement in rectangular waveguide technology is a good candidate for backward to forward radiation capability, to avoid grating lobes and to eliminate the OSB [12]. In these configurations, a waveguide is typically loaded with longitudinal radiating slots placed in the narrow wall of the waveguide. However, this results in a LWA with large lateral profile that hinders the possibility to place several of them side-by-side for the implementation of an array antenna. A ridge serpentine waveguide-based antenna without grating lobes and suitable for array implementation was presented in [15]. In this work, the waveguide was loaded with inclined radiating slots in its narrow wall. However, this structure is affected by the open stopband phenomenon. In addition, the presence of the ridge reduces the power-handling capacity of the waveguide [13]. A serpentine waveguide structure loaded with slots along the broad wall was used to feed an array of patch antennas in [3]. The open stopband was suppressed introducing reflection cancellation pillars with optimized size and distance from the slot. However, the appearance of grating lobes was unavoidable

due to the limitation on the width of the serpentine waveguide's broad wall. A waveguide antenna design that allows placing several of them side-by-side, due to its smaller width compared to serpentine waveguides, was presented in [16]. Using cylindrical posts located in the center of the waveguide, a moderate reduction of the open stopband was achieved. Also, no grating lobes were shown, except for a low-level back-lobe formed because of operating close to the cut-off frequency. Nevertheless, due to the presence of the posts, a significant part of the power is dissipated in the form of Ohmic loss, which decreases the radiation efficiency.

In this paper, a serpentine slot-waveguide LWA able to produce backward to forward radiation with open stopband suppression and without grating lobes is presented. Both unidirectional and bidirectional versions are introduced.

II. Serpentine Waveguide-based Antenna

A. Principle of Operation

The sketch of a LWA based on a serpentine rectangular waveguide loaded with transverse, non-resonant, radiating slots in the wide wall is shown in Fig. 1 (a). The distance between two consecutive slots corresponds to the length of the unit cell *d*. According to the Floquet's theorem, the propagating mode inside the proposed periodic structure can be decomposed into an infinite number of space harmonics. The phase constant of each of the *n*th space harmonics in the radiating aperture of a serpentine arrangement can be written as [12]

$$\beta_n^a = \frac{L}{d}\left(\beta_0 + \frac{2\pi n}{L}\right) \tag{1}$$

Where β_0 is the phase constant of the fundamental ($n = 0$) space harmonic that approaches the phase constant of the closed waveguide (i.e., when the loading tends to zero) and L is the meandered length of a unit cell. The phase constant of the aperture fields is increased by a factor of L/d with respect to the fields inside the waveguide.

As it is known, the illumination of the near fields determines the far field radiation pattern [2]. The angle θ (measured from the *z*-axis, within the *x*-z plane, according to Fig. 1) of the main radiated beam due to the n = −1 space harmonic can be obtained from [1]

$$sin(\theta) = \frac{\beta_{-1}^a}{k_0} \tag{2}$$

To have single-beam scanning over the entire range (i.e., only the $n = -1$ space harmonic radiates), the presence of unwanted space harmonics within the radiation region that would produce grating lobes must be avoided. This condition implies that $d < \lambda_0/2$ (λ_0 being the free-space wavelength) at the highest frequency [17]. An examination of (2) reveals that the scan rate, computed as the frequency derivative of the beam angle radiation, has a trade-off with the scanning linearity, deduced as the second frequency derivative of the beam angle. These quantities evaluated at the broadside frequency exhibit inverse and direct proportionality relationships with the period *d*, respectively. By controlling this parameter, it is possible to adjust the scan rate and the scan linearity of the structure.

B. Open Stopband Suppression

The appearance of the open stopband in periodic structures is associated with a significant amount of power from the wave travelling along the structure being reflected back to the source,

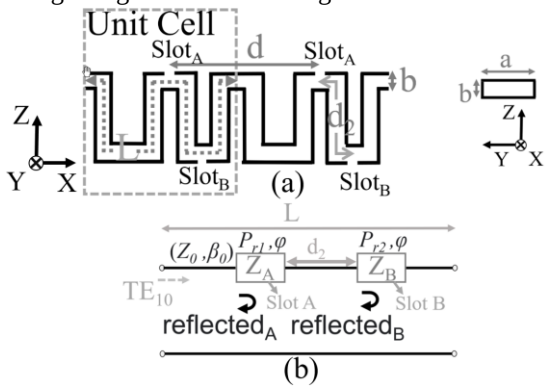

Fig. 1. (a) Sketch of the proposed leaky-wave antenna design. (b) Equivalent circuit of the unit cell.

rather than radiated, producing large mismatch. As the number of unit cells increase, the mismatch produced by the stopband becomes more visible [1]. This occurs when the broadside point is reached. To prevent the open stopband for the $n = -1$ space harmonic, each unit cell will be loaded with two identical slots, one of them placed in the top wall of the waveguide (Slot$_A$) and the other in the bottom wall (Slot$_B$), as shown in Fig. 1. Non-resonant transversal radiating slots can be modelled using the single-element impedance representation by a resistance in series with a reactance provided that the slots width is small compared with the slots length and slot lengths are less than half wavelength [14]. The resistance accounts for the radiated power through the slot (P_r) and the reactance corresponds to the reactive power. In order to avoid the wave being reflected to the source, the bottom slots must be located at a specific distance, d_2 (see Fig. 1) from the top slot so that at the beginning of the unit cell reflection from the top and bottom slots are 180º out-of-phase. Considering that only the fundamental TE$_{10}$ mode (slightly perturbed by the presence of the slots) propagates inside the waveguide with a phase constant β_0 and assuming that the reflection coefficient at the top and bottom slots are equal each other, the difference in phase delay at the beginning of the unit cell for the waves reflected at both slots will differ in two times the round-trip phase delay between the two elements, i.e., $-2\beta_0 d_2$, plus two times the additional phase, φ, due to the wave going through the top slot. These considerations lead to

$$d_2 = \frac{\lambda_g}{4}\left(1 + \frac{2\varphi}{\pi}\right) \tag{3}$$

The phase φ introduced by a single slot can be obtained from electromagnetic simulation, by comparing the phase of the S_{21} parameter of the unit cell in the case of considering only one slot and without slots, under perfect matching condition.

III. Design of the Unit Cell

A specific example is considered for an emerging broadside beam at 5 GHz from the $n = -1$ space harmonic. The material chosen for the waveguide was aluminum due to its low manufacturing cost, robustness, and good electrical conductivity. The layout of the unit cell for the proposed LWA is shown in Fig. 2. The width of the waveguide, *a*, was set to ensure the propagation of the fundamental TE_{10} mode at the operating frequency range (the cut-off wavenumber was set to be well below 5 GHz). Notice that non-standard dimensions have been used for the waveguide; the parameter *b* has been chosen to be nearly 20 times smaller than *a* to soften the limitation on the lower distance between adjacent slots and avoid the appearance of grating lobes. The dimensions of the rectangular slots ($w_s = 20$ mm and $l_s = 0.7$ mm) were chosen small enough to minimize the perturbation of the propagating TE_{10} mode. Once the slot dimensions were chosen, the amount of power radiated per unit cell can be controlled with the slot thickness, *t*. Making it lower increases the leakage rate with a minimum change in the phase constant of the guided wave. A dimensioned ramp hole (related to the parameter s_3 in Fig. 2) was used to set the slot thickness to 0.1 mm, as the manufacturer's specifications required a minimum wall width of 2 mm. To obtain the meandered length of a unit cell, *L*, and the distance between two (top and bottom) consecutive slots, d_2, the following steps were taken. First, the meandered length *L* was set to $\lambda_g = 6.92$ cm, which corresponds to the guide wavelength evaluated at the broadside frequency of 5 GHz. Next, as is shown in Fig.3 (a) the phase $\varphi = -0.19$ rad (-11^o) was obtained from electromagnetic simulation of the unit cell under perfect matching condition (using waveguide ports in the *CST Microwave Studio* software), by subtracting the phase of the S_{21} parameter without slot to the S_{21} parameter with one slot at 5 GHz [see Fig.3(a)]. Finally, the bottom slot was placed at a distance $d_2 = 15.2$ mm, calculated using (3), from the top slot and the meandered length *L* was modified to ensure that the phase of the S_{21} parameter equals -2π at the broadside frequency. As can be observed in Figure 3(b), by applying the proposed correction, the OSB is successfully eliminated, reducing the reflected power by over 15 dB compared to the non-corrected method. With the proposed geometrical arrangement, a bi-directional radiation pattern will be obtained, which may be desirable in specific applications where areas with limited space need to offer a wide coverage in wireless communications such as tunnels, long streets, or coal mines [18]-[20]. A unidirectional version of the proposed LWA is discussed in Section IV, to provide maximum design flexibility.

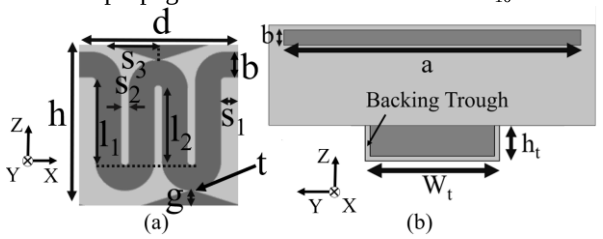

Fig. 2. (a) Unit cell cross section layout. (b) Schematic of the unidirectional version. Metallization is highlighted in light gray and the absence of metallization in dark gray. Dimensions are: a = 60 mm, b = 3.1 mm, d = 19.42 mm, h= 20.2 mm, $l_1 = 11$ mm, $l_2 = 10$, $s_1 = 2.01$mm, $s_2 = 1$ mm, $s_3 = 20.35$ mm, g = 2 mm, t = 0.1 mm, $W_t = 27$ mm, $h_t = 20$ mm.

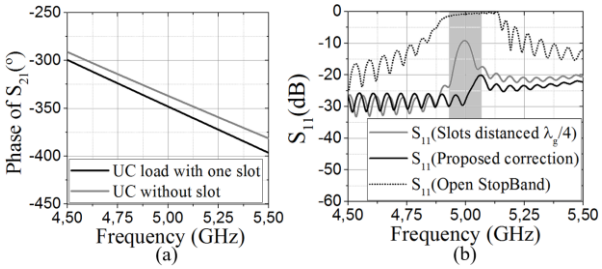

Fig. 3. (a) Phase of the transmission coefficient of a unit cell under perfect matching, load with 1 slot (black line), and without slot (grey line). (b) Comparison of 30-UC under perfect match simulation S-parameters with the slots separated by $\lambda_g/4$ (dark grey line), applying equation 3 (black line) and with OSB (black dotted line). Light grey indicates the open stopband region.

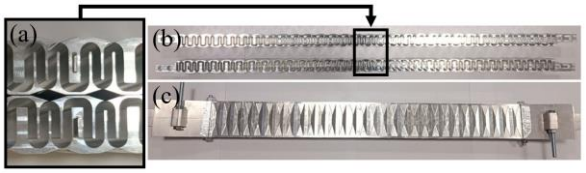

Fig. 4. Fabricated prototype. (a) Cross-sectional zoom view of the serpentine in the *xz*-plane according to Fig. 1. (b) Cross-sectional view of the total serpentine length in the *xz*-plane. (c) Full view of the device in the *xy*-plane.

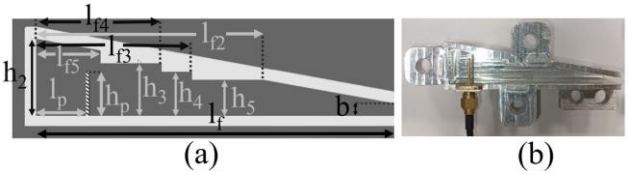

Fig. 5. (a) Layout of the matching network. Metallization is highlighted in light gray and the absence of metallization in dark gray. Dimensions are: a = 60 mm, b = 3.1 mm, $h_2 = 19$ mm, $h_p = 13$ mm, $h_3 = 13$ mm, $h_4 = 11$ mm, $h_5 = 9$ mm, $l_f = 89$ mm, $l_{f2} = 55.4$ mm, $l_{f3} = 38.5$ mm, $l_{f4} = 31$ mm, $l_{f5} = 16$ mm, $l_p = 10.5$ mm. (b) Fabricated prototype.

IV. Simulation and Experimental Results

The proposed structure is composed by 30-unit cells. The fabricated prototype is shown in Fig. 4. To feed the LWA, a coaxial-to-waveguide transition matching network based on stepped impedance and tapered transition was designed, as illustrated in Fig. 5 [21]-[22]. Very good agreement between simulated and measured *S*-parameters is achieved, as shown in Fig. 6. As can be seen, the open stop band is eliminated, and the matching level is reduced below −20 dB at the broadside frequency. The unidirectional design [see Fig.2 (b)]is based on the same structure, with a backing trough placed on the bottom surface along the *x*-axis, in a similar way as it was done in [23]. It consists of a long metallic cavity that can be thought as a waveguide operating well below the cutoff frequency of the first dominant mode. It can be appreciated that there are no significant changes due to the presence of the backing trough, and the open stop band is also eliminated showing a matching level below −20 dB at the broadside frequency. A comparison between the measured and analytical scanning angle is shown in Fig. 7. The analytical angle was computed from (2), where β_0 was obtained from an electromagnetic simulation of the unit

cell. It can be appreciated that very good matching is achieved showing a linear dependence of the radiation angle and the frequency, which is useful for frequency-scanned frequency-modulated continuous wave (FMCW) radars [16] and other scanning systems [24]. The simulated and measured (in an anechoic chamber environment) normalized radiation pattern in the E plane show

top and bottom gains. This is mainly attributed to differences in the dimensions of the top and bottom slots due to manufacturing tolerances. An increase on the gain (of 2 dB average) was observed for the unidirectional antenna compared to the bidirectional one, which shows that most of the back radiation is recovered by the backing trough. The simulated radiation efficiency ranges from 83% to 97% for the bidirectional structure and from 72% to 93% for the unidirectional version.

Ref	Type	Bandwidth (GHz)	Radiation Efficiency [%]	Scanning angle (º)	Gain (dBi)	Grating lobes	OSB	Antenna length (λ_0)
[22]	Corrugated PPW	28~40	>80	-42.5~5.5	9.1~14.1	No	Mitigated	9.4
[3]	Array antenna	230~245	60	-24~24.5	29~30	Yes	Eliminated	34
[16]	Waveguide LWA	27~34.7	54~90	-38~27	11.5~19	No	Mitigated	27.6
[15]	SSDA	9.7~10.3	<60	-23~16	12~20	No	Yes	22.8
[25]	Waveguide LWA	30.5-40	40~75	-29~31	16~19.5	No	Mitigated	31
This work	SSAA (Bidirectional 30UC)	4.3~5.7	83~97 (sim)	-42~34	10~15.5	No	Eliminated	9.7
	SSAA (Unidirectional 30UC)	4.3~5.7	72~93 (sim)	-43~36	11.2-16.4	No	Eliminated	9.7

TABLE I Performance comparison with other air-filled FSAs

The proposed design results in a low lateral profile LWA that

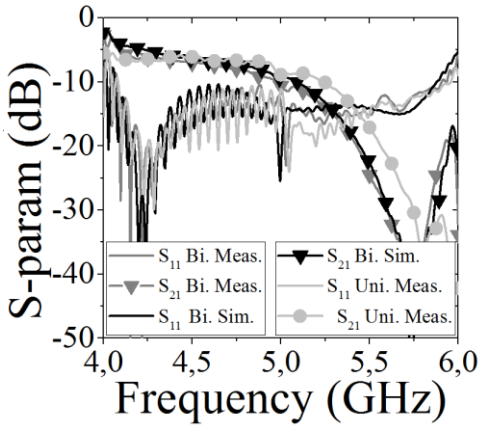

Fig. 6. Comparison antenna simulation and measured S-parameters in different configurations.

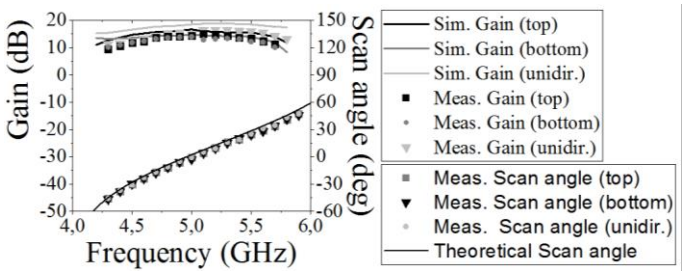

Fig. 7. Measured and simulated gain and scan angle for the proposed bidirectional and unidirectional LWAs.

good agreement in both versions (see Fig. 8). As can be appreciated, the unidirectional LWA works well, suppressing the back radiation below −18 dB. As the frequency sweeps from 4.3 to 5.7 GHz, the main beam steers from −35° to 42° in both structures, with the beam directed to broadside at 5 GHz. The measured gains for both unidirectional and bidirectional versions are depicted in Fig. 7 showing a maximum value of 16.5 dB and 15.5 dB, respectively. The structure with a bidirectional pattern exhibits a significant difference between

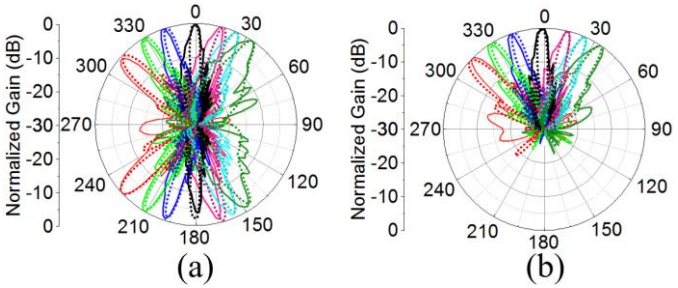

Fig. 8. Normalized measured (solid lines) and simulated (dotted lines) radiation pattern in the E plane for (a) the bidirectional LWA and (b) the unidirectional version. The considered frequencies are 4.3 GHz (red), 4.5 GHz (light green), 4.7 GHz (dark blue), 5 GHz (black), 5.3 GHz (magenta), 5.5 GHz (cyan), and 5.7 GHz (dark green).

allows to place several of them side-by-side for the implementation of an array antenna. In Table 1 a frequency scan antenna features comparison is shown. In this table, the open stopband is considered as rejected and mitigated when the reflection coefficient is below – 15 dB and – 8 dB at broadside radiation frequency respectively. Compared to other designs, the proposed prototype antenna offers a high scanning range, high radiation efficiency, and eliminates both grating lobes and OSB.

V. Conclusions

In this paper, a novel LWA design based on a meandered rectangular waveguide loaded with transversal slots has been proposed. Both unidirectional and bidirectional versions of the antenna have been presented. This structure is a periodic leaky-wave antenna able to produce backward, broadside and forward radiation from its fundamental TE_{10} mode. The introduced prototypes have been successfully tested, exhibiting a backward-to-forward scanning range from −35° to 42° in both structures, with the beam directed to broadside at 5 GHz. Effective open stop band suppression has been demonstrated showing a matching level below −20 dB at the broadside

frequency. The maximum measured gains are 15.5 dB and 16.5 dB for the bidirectional and unidirectional LWAs, respectively. The antenna simulated radiation efficiency changes from 83% to 97% for the bidirectional structure and from 72% to 93% for the unidirectional version. Both LWAs have a narrow lateral profile that allows for the implementation of an array antenna making them suitable for 2D scanning (e.g., frequency scanning along the longitudinal direction and electronic scanning along the transverse direction).

ACKNOWLEDGMENT

This research was supported by the TEC2016-75650-R (funded by the Spanish MCIN/AEI/10.13039/501100011033 and FEDER). Álvaro Jaque Jiménez acknowledges MINECO for supporting his research activity through the FPI grant BES-2017-081387.

REFERENCES

[1] J. L. Volakis, *Antenna Engineering Handbook*, USA, NY, New York:McGraw-Hill, 2007.

[2] C. A. Balanis, *Modern Antenna Handbook*, Hoboken, NJ, USA:Wiley, 2008.

[3] K. Sarabandi, A. Jam, M. Vahidpour, and J. East, "A Novel Frequency Beam-Steering Antenna Array for Submillimeter-Wave Applications," in *IEEE Transactions on Terahertz Science and Technology*, vol. 8, no. 6, pp. 654-665, Nov. 2018, doi: 10.1109/TTHZ.2018.2866019.

[4] Young Ju Lee, Junho Yeo, R. Mittra, and Wee Sang Park, "Application of electromagnetic bandgap (EBG) superstrates with controllable defects for a class of patch antennas as spatial angular filters," in *IEEE Transactions on Antennas and Propagation*, vol. 53, no. 1, pp. 224-235, Jan. 2005, doi: 10.1109/TAP.2004.840521.

[5] J. Liu, et al., "A simple technique for open-stopband suppression in periodic leaky-wave antennas using two nonidentical elements per unit cell", *IEEE Trans. Antennas Propag.*, vol. 66, no. 6, pp. 2741-2751, Jun. 2018, doi: 10.1109/TAP.2018.2819701.

[6] A. J. Mackay and G. V. Eleftheriades, "Meandered and Dispersion-Enhanced Planar Leaky-Wave Antenna With Fast Beam Scanning," in *IEEE Antennas and Wireless Propagation Letters*, vol. 20, no. 8, pp. 1596-1600, Aug. 2021, doi: 10.1109/LAWP.2021.3091979.

[7] S. Paulotto, et al. "A novel technique for open-stopband suppression in 1-D periodic printed leaky-wave antennas*", IEEE Trans. Antennas Propag*., vol. 57, no. 7, pp. 1894-1906, Jul. 2009, doi: 10.1109/TAP.2009.2019900.

[8] D. Comite et al., "A dual-layer planar leaky-wave antenna designed for linear scanning through broadside", *IEEE Antennas Wireless Propag. Lett*., vol. 16, pp. 1106-1110, 2016, doi: 10.1109/LAWP.2016.2639586.

[9] P. Baccarelli, et al., "Open-stopband suppression via double asymmetric discontinuities in 1-D periodic 2-D leaky-wave structures", *IEEE Antennas Wireless Propag. Lett*., vol. 18, no. 10, pp. 2066-2070, Oct. 2019, doi: 10.1109/LAWP.2019.2937473.

[10] X.-L. Tang, "Continuous beam steering through broadside using asymmetrically modulated Goubau line leaky-wave antennas", *Sci. Rep*., vol. 7, 2017, 10.1038/s41598-017-12118-8.

[11] M. Kuznetcov et al., "Half-Annular Leaky-Wave Antenna With Suppressed Open Stopband: Design and Experimental Testing," in *IEEE Antennas and Wireless Propagation Letters*, vol. 22, no. 5, pp. 1204-1208, May 2023, doi: 10.1109/LAWP.2023.3236614.

[12] A. A. Oliner, "1963 Short Course on Microwave Field and Network Techniques" Brooklyn, Polytechnic Institute of Brooklyn, Tuesday, June 4, 1963.

[13] David M. Pozar, *Microwave Engineering*, Hoboken, NJ :Wiley, 2012.

[14] Richard C. Johnson, *Antenna Engineering Handbook*, third eddition, USA, NY, New York:McGraw-Hill, 2007

[15] W. Yin *et al*., "Frequency Scanning Single-Ridge Serpentine Dual-Slot-Waveguide Array Antenna," in *IEEE Access*, vol. 8, pp. 77245-77254, 2020, doi: 10.1109/ACCESS.2020.2989318.

[16] A. Ohadi and G. V. Eleftheriades, "Slotted Waveguide Frequency-Scanned Slow-Wave Antenna With Reduced Sensitivity of the Closed Stopband at Millimeter-Wave Frequencies," in *IEEE Access*, vol. 10, pp. 27783-27793, 2022, doi: 10.1109/ACCESS.2022.3152905.

[17] M. Guglielmi and G. Boccalone, "A novel Theory for Dielectric-Inset Waveguide Leaky-Wave Antennas," in *IEEE Transactions on Antennas and Propagation*, vol. 39, no. 4, pp. 497-504, April 1991.

[18] F. Ge, H. Zhao, S. Li and X. Yin, "Bidirectional Scanning Antenna Based on Surface Wave Mode," in *IEEE Antennas and Wireless Propagation Letters*, vol. 21, no. 8, pp. 1592-1596, Aug. 2022, doi: 10.1109/LAWP.2022.3174879.

[19] Z. L. Ma and L. J. Jiang, "One-Dimensional Triple Periodic Dual-Beam Microstrip Leaky-Wave Antenna," in *IEEE Antennas and Wireless Propagation Letters*, vol. 14, pp. 390-393, 2015, doi: 10.1109/LAWP.2014.2365394.

[20] L. Liu, Z. Zhang, Z. Tian and Z. Feng, "A Bidirectional Endfire Array With Compact Antenna Elements for Coal Mine/Tunnel Communication," in *IEEE Antennas and Wireless Propagation Letters*, vol. 11, pp. 342-345, 2012, doi: 10.1109/LAWP.2012.2191383.

[21] W. Yi, E. Li, G. Guo and R. Nie, "An X-band coaxial-to-rectangular waveguide transition," *IEEE International Conference on Microwave Technology & Computational Electromagnetics*, Beijing, China, 2011, pp. 129-131, doi: 10.1109/ICMTCE.2011.5915181.

[22] Z. Liu, H. Lu, J. Liu, S. Yang, Y. Liu and X. Lv, "Compact Fully Metallic Millimeter-Wave Waveguide-Fed Periodic Leaky-Wave Antenna Based on Corrugated Parallel-Plate Waveguides," in *IEEE Antennas and Wireless Propagation Letters*, vol. 19, no. 5, pp. 806-810, May 2020, doi: 10.1109/LAWP.2020.2980993.

[23] A. Grbic and G. V. Eleftheriades, "Leaky CPW-based slot antenna arrays for millimeter-wave applications," in *IEEE Transactions on Antennas and Propagation*, vol. 50, no. 11, pp. 1494-1504, Nov. 2002, doi: 10.1109/TAP.2002.804259.

[24] M. Skolnik, Radar Handbook, New York, NY, USA:McGraw-Hill, 2008.

[25] Q. Yang, X. Zhao and Y. Zhang, "Design of CRLH Leaky-Wave Antenna With Low Sidelobe Level," in *IEEE Access*, vol. 7, pp. 178224-178234, 2019, doi: 10.1109/ACCESS.2019.2958496.